







RADIOCARBON DATING OF MORTAR FROM THE AQUEDUCT IN SKOPJE

Andreja Sironić^{1*}  • Damir Borković¹ • Jadranka Barešić¹  • Ines Krajcar Bronić¹  • Alexander Cherkinsky²  • Ljiljana Kitanovska³ • Vjekoslav Štrukil¹  • Lidija Robeva Čukovska⁴ 

¹Ruder Bošković Institute, Bijenička c 54, Zagreb, Croatia

²Center for Applied Isotope Studies, University of Georgia, Athens, GA, USA

³National Institution Conservation Centre, Skopje, R Macedonia

⁴NI National Conservation Centre – Central Chemical Laboratory, Skopje, R. North Macedonia

ABSTRACT. The Aqueduct is one of the city landmarks of Skopje, Republic of North Macedonia. It was part of a water-supply system, with a total original length of about 10 km, while its surface remains are about 385 m long. The age of the Aqueduct is not known—several hypotheses place it to periods between the 6th and 16th centuries. Six mortar samples from different positions of the eastern façade were taken for radiocarbon (¹⁴C) dating. In order to extract only the carbon associated to the time of building, three strategies for sample preparation were used: (1) mechanical separation of lime lumps formed during mortar hardening (2) selection on the basis of particle size and the ability to suspend in water induced by ultrasonic shock, and (3) collection of two gas CO₂ fractions produced from the same bulk in reaction with acid. Characterization of fractions was performed by isotopic carbon composition and FTIR-ATR analyses. The most plausible results were obtained from lime lump fractions that were dated in the timeframe of 15th to 17th century.

KEYWORDS: AMS, Aqueduct in Skopje, mortar, radiocarbon dating.

INTRODUCTION

The Aqueduct is one of the Landmarks of Skopje, located in the northwestern part of Skopje, the capital of the Republic of North Macedonia. Originally part of a water-supply system (in use until 1915), with a total length of about 10 km, in general NE to SW direction, the monument as it stands today is more than 380 m long, with two access ramparts, 53 pillars, 54 base vaults, and 42 smaller vaults above the pillars. It is the only preserved monument of this type in Macedonia.

The historical development of the Aqueduct cannot be traced with certainty. There are three hypotheses about the timing of its construction. (1) The Aqueduct was built during the urbanization of Skopje (527–554 AD) by the Byzantine Emperor Justinian I, who was born in the vicinity of Skopje. This is supported by the notes of Procopius Caesariensis (a 6th-century historian), who wrote that along the beautiful buildings, castles, etc., a water supply system for the town of Justiniana Prima was built. (2) The Aqueduct was built in the 15th century (Kumbaradži-Bogojević 1998) by Mustafa Pasha who was responsible for a few other buildings in Skopje. (3) It was built in the 16th century (Balabanov et al. 1980; Petru 1998) as a part of Isa-Beg's water supply system.

In 2014, a comprehensive study of the Aqueduct was undertaken, and among other physico-chemical analyses, 6 mortar samples were submitted for radiocarbon (¹⁴C) dating. The analyses would hopefully resolve the question of the timing of the Aqueduct construction, or various phases of its construction.

Absolute mortar dating is often needed in archeological studies, and attempts to date mortar by ¹⁴C are as old as the radiocarbon dating itself (Labeyrie and Delibrias 1964; Baxter and Walton 1970; a review paper Hale et al. 2003). Mortar can be ¹⁴C-dated by isolating the atmospheric

*Corresponding author. Email: asironic@irb.hr.

carbon fixed in mortar binder at the time the mortar was applied. However, results often are compromised with dead carbon contamination originating from unreacted limestone during the preparation of quick lime or as a part of the aggregate. Also, a sample can be contaminated with secondary carbonates from the environment (Lindroos et al. 2007; Nonni et al. 2018) and crystallization connected with capillary rise from ground water or rain water through older limestone leading to the recrystallization (Michalska and Czernik 2015), with atmospheric carbon which was introduced later, due to later fire events (Lindroos et al. 2012), or delayed/stopped and re-started carbonization (e.g. Van Balen 2005; Hajdas et al. 2017). It can take decades for the hardening process to end (Sonninen et al. 1989; Van Strydonck and Dupas 1991; Michalska et al. 2017). Due to these problems, several fractions need to be analyzed, making mortar dating economically challenging. Instructions on the optimal fraction selection and data interpretations are discussed in Lindroos et al. (2018). Characterization of mortar is often applied, usually with basic petrographic, SEM, XRD, TGA, FTIR, EPR, and elemental analyses (Nawrocka et al. 2005; Chu et al. 2008; Ortega et al. 2008, 2012; Szczepaniak et al. 2008; Goslar et al. 2009; Nawrocka et al. 2009; Poduska et al. 2012; Nonni et al. 2013; Fabbri et al. 2014; Kabacińska et al. 2014; Hayen et al. 2016, 2017) as well as $\delta^{13}\text{C}$ and $\delta^{18}\text{O}$ composition of carbonate aggregates (Van Strydonck et al. 1986, 1989; Michalska et al. 2015).

Lime lumps are homogenous white spots of varying size that may form upon mortar production or before the mortar is mixed with an aggregate and used (Lindroos et al. 2007). Lime lumps can be used for dating either in whole, after sequential dissolution, or treated with ultrasonic shock (Pesce et al. 2009; Pesce and Ball 2012; Lindroos et al. 2014, 2018; Ringbom et al. 2014; Carmine et al. 2015).

If lime lumps are not available, selections of fractions based on grain size are applied (e.g. Michalska Nawrocka et al. 2007; Heinemeier et al. 2010; Ortega et al. 2012), sometimes combined with the rate of hydrolyses decomposition/leaching reactions of each fraction (Michalska and Czernik 2015; Michalska et al. 2017). Further, the CryoSonic/Cryo2Sonic procedure selects the portion that forms flocculates during treatment in ultrasonic water-bath (Nawrocka et al. 2005; Marzaioli et al. 2013; Nonni et al. 2013, 2018).

In this first attempt to absolutely date the construction of the Aqueduct in Skopje, we combined two methods for mortar dating: lime lumps and the CryoSonic procedure combined with acid leaching.

MATERIALS AND METHODS

Sampling Locations

Sampling was conducted on July 28, 2017, at the site of the monument (Figure 1) near Skopje (Cfa climate type, average annual temperature 13°C, summer 24°C, and winter 2°C). The sample locations were previously selected with the intention of comparing the mortar used in the foundation of the monument with the mortar used in the other constructive parts of the Aqueduct. Such a sampling strategy was based on the hypothesis that the foundation mortar is an original or the oldest mortar. For that purpose, a total of 6 samples were collected from different locations of the Aqueduct, which are demonstrated in Table 1 and Figure 1. The weight of each sample was 150–200 g.



Figure 1 Sampling locations and macrophotographs of samples: (A) a drawing of the overall length (387.98 m) of the Aqueduct and the distance between the sampling locations, along the monument with location of the Aqueduct (drop-like symbol) in Macedonia and location of Macedonia in Europe (inset figure); (B) part of the northern rampart and details of the sampling positions: Aq1 foundation mortar and Aq2 plumbing channel; (C) the ruined Pillar S48 and detail of the sampling position: Aq3-mortar core from the walled opening between the arches; (D) Pillar S38 and details of the sampling positions: Aq4-mortar joint between the bricks (inner layer), Aq5-mortar joint between brick (external layer) and Aq6-mortar joint between the stones/bricks, taken from the surface (external layer); (E) macrophotographs of samples.

Table 1 Sampling locations and positions.

Sample	Sampling locations	Sampling positions
Aq1	Eastern facade, the foundation of the northern rampart	Mortar from the surface of the masonry (external layer)
Aq2	Eastern façade, plumbing channel	Mortar at a depth of about 10 cm (inner layer)
Aq3	Eastern facade of the partly ruined Pillar S48, walled openings between the arches	Mortar core at a depth of about 15 cm (inner layer, the surface was broken to reach this part)
Aq4	Eastern facade, Pillar S38, at about 100 cm height	Mortar core of the bottom part; from a hole about 30 cm deep, used to place a wooden beam
Aq5	Eastern facade, southern side of the arch of the relief opening in the upper part of the Pillar S38	Mortar joint between bricks (external layer)
Aq6	Southern face of the Pillar S38 bottom, at about 40 cm height	Mortar joint between the stones/bricks, taken from the surface (external layer)

Sample Preparation and Analyses

Mortar samples had a negative reaction when tested on pH with phenolphthalein solution, i.e., their pH was lower than 8 (Ringbom et al. 2008). The surface of the samples was grey, and a few millimeters beneath the surface the samples were white, apart from sample Aq2, which was brick-brown-red throughout. The surface of Aq4 sample had a dark coating. All the samples had a white binder, visible carbonaceous lime lumps, and coarse aggregate, with some limestone aggregate, apart from Aq2, which had much finer aggregate, brick-red filler with some visible white lime lumps (Figure 1E). Lime lumps were macroscopically well-defined in all the samples. Since the size of the aggregates were coarse, and some carbonaceous (limestone) aggregates were found in the samples, implying that for the aggregates were not finely crushed during the mortar production, the possibility of dead carbon inside the *Lime* finding as initial precipitating particle was considered to be minimal and the *Lime* lumps were found to be the most reliable part for dating. In the Laboratory the mortars were subsampled by use of chisel and hammer: 2–3 cm below the surface to obtain 10–15 g of the subsample.

The CryoSonic method was applied for all samples to mechanically select mortar fractions on the basis of particle size (Nawrocka et al. 2005; Marzaioli et al. 2013; Michalska et al. 2017).

Part of subsamples (~5 g) was broken cryogenically by alternate cooling (dipping into liquid nitrogen) and heating (in the oven at 80°C, for 20 min), for at least 4 cycles, and then gently crushed with a hammer. Samples were wet-filtered with ultrapure water (UPW) on a 450- μ m sieve. Portions larger than 450 μ m were optically inspected for lime lumps and two fractions were separated: *Lime lumps*—white powdery lumps assigned to the time to the building (Pesce and Ball 2012), and *Rest*—all other. After the cryobreaking, the *Lime lumps* were found in samples Aq3 to Aq6. They ranged in size from 1 mm (Aq3) to 5 mm (Aq5 and Aq6) in diameter.

Portions finer than 450 μ m were treated in UPW in ultrasonic bath for 30 min. Immediately after ultrasonication, suspended fractions (*Susp*) were decanted and centrifuged at 2662 g for 5 min and along with the precipitated fraction (*Sediment*) were oven dried at 80°C over night. All fractions were analyzed by FTIR-ATR.

CO₂ from mortar fractions of *Rest*, *Lime lumps* and *Sediment* was produced by 4 % HCl. From *Susp* fractions 85 % H₃PO₄ at 25°C was used, and CO₂ was collected in two consecutive fractions: *Susp-1*, the first 60 seconds of the reaction, and *Susp-2*, until the end of the reaction. If there were not enough gas produced for the carbon isotope analyses, the two CO₂ fractions were merged into one: *Susp-1 + 2*

A portion of obtained CO₂ was sealed in a pyrex glass tube for δ¹³C analyses on Isotope ratio mass spectrometer (IRMS), and another portion was Zn reduced to graphite for ¹⁴C Accelerator mass spectrometer (AMS) analyses at the Ruđer Bošković Institute (RBI) (Krajcar Bronić et al. 2010; Sironić et al. 2013). The IRMS and AMS ¹⁴C analyses were done at the Center for Applied Isotope Studies (CAIS), Athens, GA, USA.

Samples Aq1 *Susp-1 + 2*, Aq3 *Susp-1 + 2* and Aq3 *Lime lump* (Z-6510, Z-6516, and Z-6731; Table 2) were prepared at CAIS as bulk CO₂ produced by hydrolysis with 85 % H₃PO₄ at 20°C.

Measured δ¹³C values are expressed in per mil relative to VPDB and ¹⁴C values are normalized to δ¹³C -25 ‰ and expressed as age before present (BP) or as a ¹⁴C in percent modern carbon (pMC; Mook and van der Plicht 1999). ¹⁴C conventional ages were calibrated by OxCal v4.2.4 software (Bronk Ramsey 2016; OxCal v4.3.2, see Bronk Ramsey 2017; r:5) and IntCal13 calibration curves (Reimer et al. 2013).

Fourier-transform infrared attenuated total reflection (FTIR-ATR) spectra were recorded using a PerkinElmer UATR Two spectrometer in the range 450 cm⁻¹ to 4000 cm⁻¹, with a spectral resolution of 4 cm⁻¹ and total of 8 scans accumulated. Automatic ATR correction algorithm was applied to account for relative intensity shift in the collected FTIR spectra. The ν₂/ν₄ peak intensity ratio corresponding to the out-of-plane bending (ν₂ = 873 cm⁻¹) and in-plane bending (ν₄ = 712 cm⁻¹) of calcite was calculated by drawing the baseline between the closest minima on the sides of these two peaks and reading the peak intensity values (Chu et al. 2008).

A chi-square test was used to evaluate the difference between measured values with a declared significance level α=0.05.

RESULTS

FTIR-ATR Analyses—Mortar Characterization

Qualitative FTIR-ATR analyses of all samples (Figure 2) confirmed the presence of calcite as the major component, evidenced by the characteristic peaks positioned at 712, 873, 1408, 1796, and 2513 cm⁻¹ (Chu et al. 2008; Poduska et al. 2012). Quartz, clay (kaolinite) and/or gypsum were also identified in most fractions (Figure 2). Based on the intensity of characteristic quartz signals at 695, 779, 798, 1082, and 1163 cm⁻¹, it was found in Aq1 and Aq4 *Rest* samples and also in small amount in Aq1 and Aq2 *Sediments*. Absorption bands in Aq6 *Rest* fraction at 3526, 3400, 1622, 1107, 1006, 667, and 599 cm⁻¹ indicate the presence of gypsum, which is also found in Aq3 *Rest* fractions. *Lime lump* fractions Aq4–Aq6 seem to be made of pure calcite while Aq3 *Lime lump* fraction also contains signals for kaolinite clay (broad absorption at 1009–1023 and 3200–3600 cm⁻¹). Kaolinite bands are present in all Aq1–Aq6 *Sediment* and *Susp* fractions as well, suggesting that the binders of analyzed mortars were

made of carbonaceous clay-containing minerals. Overall, all four fractions of each mortar appear as similar in their chemical composition, particularly *Susp* and *Lime lump* fractions.

The ν_2/ν_4 ratios (at 873 and 712 cm^{-1} , respectively) of the corresponding CaCO_3 vibration intensities for different samples were found in the range from 4.4–5.3 for *Sediment* fractions, 4.2–6.2 for *Lime lump* fractions, 5.0–6.6 for *Susp* fractions and 4.1–5.0 for *Rest* fractions. In comparison with Carrara marble as the pure geogenic calcite with the ν_2/ν_4 ratio of 2.3, elevated ν_2/ν_4 values for the studied samples suggest their anthropogenic origin (Chu et al. 2008).

Isotope ^{13}C and ^{14}C Analyses

The results of ^{14}C and ^{13}C measurements are presented in Table 2. $\delta^{13}\text{C}$ values are similar within different fractions of individual mortar sample. Samples Aq1 and Aq4 have the most negative $\delta^{13}\text{C}$ values, samples Aq2, Aq5, and Aq6 similar values and Aq3 has the most positive $\delta^{13}\text{C}$ values for *Sediment* and *Susp* fractions, but similar to Aq5 and Aq6 for *Lime lumps* fraction. In each case where there were available both *Susp*-1 and *Susp*-2 fractions, $\delta^{13}\text{C}$ for *Susp*-1 fraction is lower than for *Susp*-2 (Table 2). This is observed in case of consecutive fractions and explained as a kinetic effect (Van Strydonck et al. 1986; Lindroos et al. 2007): in the reaction with acid, the lighter carbon isotope reacts first, and then the heavier. $a^{14}\text{C}$ values of *Susp*-1 and *Susp*-2 fraction of mortar Aq6 are statistically the same which supports the presumption of the mentioned $\delta^{13}\text{C}$ kinetic effect.

In general, for all samples with the exception of Aq4, the highest $a^{14}\text{C}$ values within each sample were observed in *Lime lumps* (if available) followed by *Susp*-1 fractions, and the lowest values in *Rest*. Only in the case of Aq3 the age of *Susp* fraction was in agreement with the *Lime lumps* fraction. For two samples, Aq5 and A6, *Susp* fractions were ~ 100 ^{14}C yr older than *Lime lumps*, and for Aq4 ~ 100 years younger. This leads to a conclusion that the *Susp* fractions are not reliable in dating, but are not far from the true age.

DISCUSSION

Correlations of $\delta^{13}\text{C}$ to $a^{14}\text{C}$

$a^{14}\text{C}$ to $\delta^{13}\text{C}$ correlations (Figure 3) pinpoint to the dead-carbon or to biogenic carbon contamination. Dead carbon contamination would be visible as a trend toward lower $a^{14}\text{C}$ and higher $\delta^{13}\text{C}$ values. We assumed for the dead-carbon contamination to be minimal or absent in *Lime lumps*, intermediate in *Susp*-1, *Susp*-2 and *Sediment*, and the most contaminated part would be *Rest*. Trends for $\delta^{13}\text{C}$ and $a^{14}\text{C}$ fractions of samples Aq1, Aq2, and Aq5 (Figure 3) show such features pointing to dead carbon contamination.

Aq3 is the only sample where $a^{14}\text{C}$ for *Susp* and *Lime lumps* fractions are statistically the same. The *Sediment* fraction has lower $a^{14}\text{C}$ than *Lime lumps* and *Susp* fractions indicating the dead-carbon contamination in *Sediment*. Aq3 *Sediment* and *Susp*-1 + 2 fractions $\delta^{13}\text{C}$ are also similar, while $\delta^{13}\text{C}$ for *Lime lumps* is lower (-11.6‰). This could be associated with the kinetic effect rather than with the influence of dead-carbon contamination. Longer slaking process creating the lime putty (hydroxylation of quick lime) results in lower $\delta^{13}\text{C}$ values of precipitated carbonates (Ambers 1987). The lowest $\delta^{13}\text{C}$ values for large *Lime lumps* can be explained by their formation during delayed slaking. In contrast, *Susp* fraction consists of

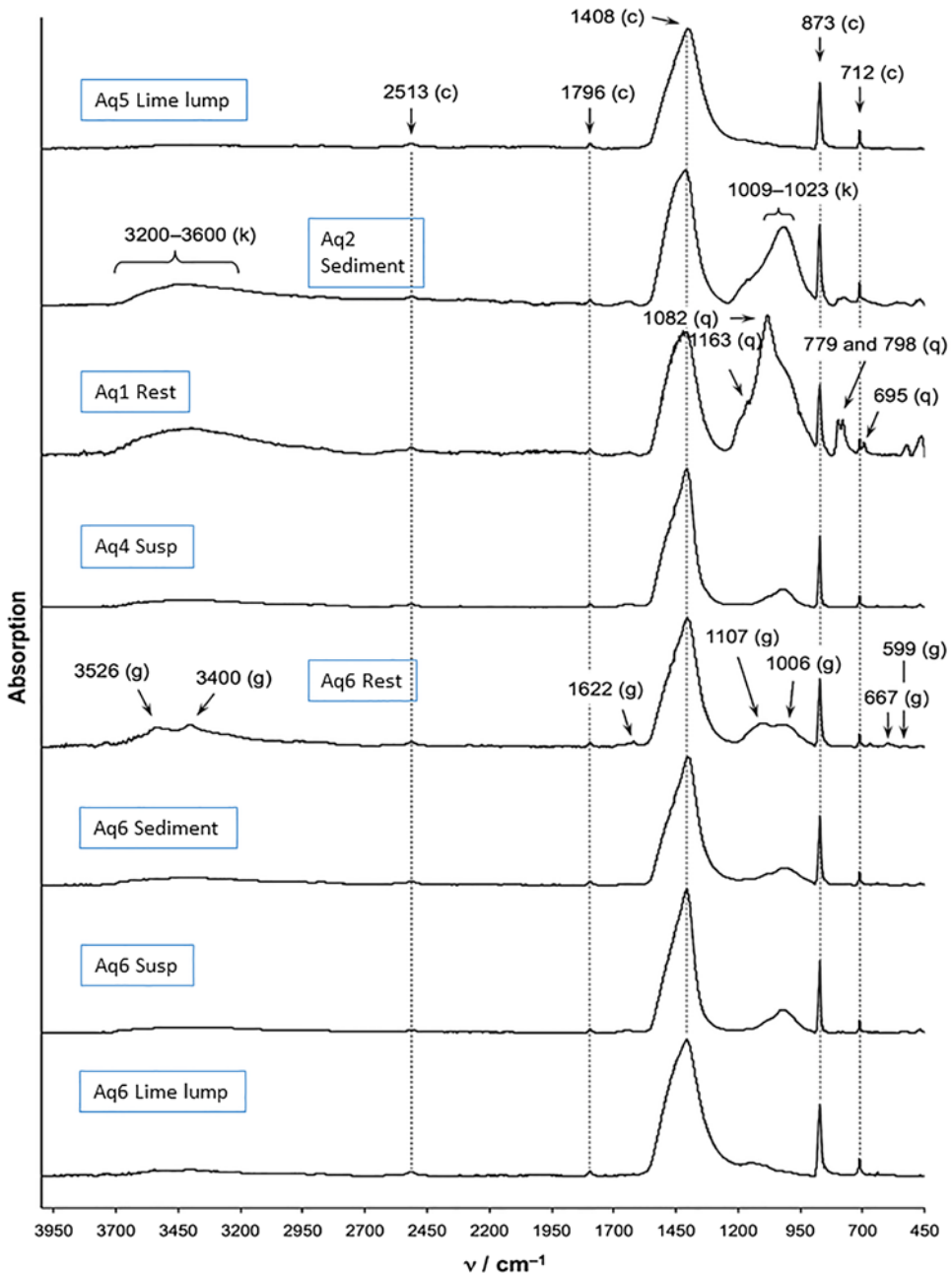


Figure 2 FTIR-ATR spectra for sample Aq5 *Lime lump*, Aq2 *Sediment*, Aq1 *Rest*, Aq4 *Susp.*, Aq6 *Rest*, Aq6 *Sediment*, Aq6 *Susp.*, and Aq6 *Lime lump* fractions (from top to bottom): (c) calcite, (k) kaolinite, (g) gypsum, (q) quartz; fractions: *Rest*- > 450 μm -bulk; *Sediment*- < 450 μm , precipitate after ultrasonification, *Susp*- < 450 μm , suspended part, (-1, CO₂ extracted within 60'; -2, CO₂ extracted till the end of reaction; -1 + 2, CO₂ extracted as bulk); *Susp* and *Lime lumps* fractions of other samples are similar to those presented here.

Table 2 Measured $a^{14}\text{C}$ and $\delta^{13}\text{C}$ for all analyzed fractions of mortar samples from Aq1 to Aq6: Laboratory Z represents a sample identification number at RBI, UGAMS is a sample identification number at CAIS, $a^{14}\text{C}$ expressed in pMC, conventional ^{14}C age in BP, $\delta^{13}\text{C}$ in per mill with σ of 0.1‰; fractions: *Rest*- > 450 μm -bulk; *Sediment*- < 450 μm , precipitate after ultrasonification, *Susp*- < 450 μm , suspended part, (-1, CO_2 extracted within 60', -2, CO_2 extracted till the end of reaction:-1 + 2, CO_2 extracted as bulk), *Lime lump*- > 450 μm , white powdery lumps.

Sample Name	Z	UGAMS	$a^{14}\text{C}$ (pMC)	Conventional ^{14}C age (BP)	$\delta^{13}\text{C}$ (‰)
Aq1 <i>Rest</i>	6511	31261	87.66 ± 0.23	1057 ± 21	-18.46
<i>Sediment</i>	6512	31262	90.26 ± 0.24	823 ± 21	-21.42
<i>Susp</i> -1	6510	31260	Sample lost on preparation		-20.86
<i>Susp</i> -2		31280	Not available		-19.94
<i>Susp</i> -1 + 2 (CAIS)	6510	36912	92.98 ± 0.28	584 ± 24	-20.60
<i>Lime lump</i>	Not found				
Aq2 <i>Rest</i>	Not measured				
<i>Sediment</i>	6509	31259	92.48 ± 0.24	628 ± 20	-11.44
<i>Susp</i> -1	6508	31258	95.70 ± 0.26	353 ± 21	-12.73
<i>Susp</i> -2	Not available				
<i>Lime lump</i>	Not found				
Aq3 <i>Rest</i>	Not measured				
<i>Sediment</i>	6517	36897	92.36 ± 0.23	638 ± 19	-7.88
<i>Susp</i> -1 + 2 (CAIS)	6516	36913	93.47 ± 0.29	541 ± 24	-7.33
<i>Lime lump</i> (CAIS)	6731	36914	93.57 ± 0.25	534 ± 20	-11.55
Aq4 <i>Rest</i>	Not measured				
<i>Sediment</i>	6519	31265	109.30 ± 0.29	Modern sample	-24.86
<i>Susp</i> -1	6518	31264	97.34 ± 0.26	216 ± 21	-25.74
<i>Susp</i> -2	Not available				
<i>Lime lump</i>	6533	31274	94.02 ± 0.25	495 ± 21	-28.42
Aq5 <i>Rest</i>	Not measured				
<i>Sediment</i>	6529	31276	93.65 ± 0.26	527 ± 22	-10.22
<i>Susp</i> -1 + 2	6531	31271	94.96 ± 0.26	415 ± 21	-9.96
<i>Lime lump</i>	6530	31270	95.71 ± 0.26	352 ± 21	-11.08
Aq6 <i>Rest</i>	6532	31272	91.69 ± 0.25	697 ± 21	-12.05
<i>Sediment</i>	6523	31268	93.69 ± 0.25	523 ± 21	-11.16
<i>Susp</i> -1	6520	32358	95.19 ± 0.29	395 ± 24	-11.34
<i>Susp</i> -2	6521	32352	94.99 ± 0.17	412 ± 22	-10.65
<i>Lime lump</i>	6522	31275	96.34 ± 0.26	299 ± 21	-10.78

(CAIS) = CO_2 production and graphite preparation done at CAIS.

flocculates formed on the surface, probably immediately after mortar application, and was influenced by quicker slaking process and would express higher $\delta^{13}\text{C}$ values.

Modern $a^{14}\text{C}$ value of the Aq4 *Sediment* fraction implies delayed/stopped and re-started carbonization. All dated fractions show very low $\delta^{13}\text{C}$ (-28‰ to -24‰) which could be associated with: fire-damaged mortar (Lindroos et al. 2012) or to a long slaking process (Ambers 1987). The sample Aq4 had dark coating on its surface, which was FTIR-ATR analyzed showing absorption bands at 2915 and 2848 cm^{-1} characteristic of mineral tar, suggesting that this mortar had been fire damaged. Since *Lime lump* has very low $\delta^{13}\text{C}$

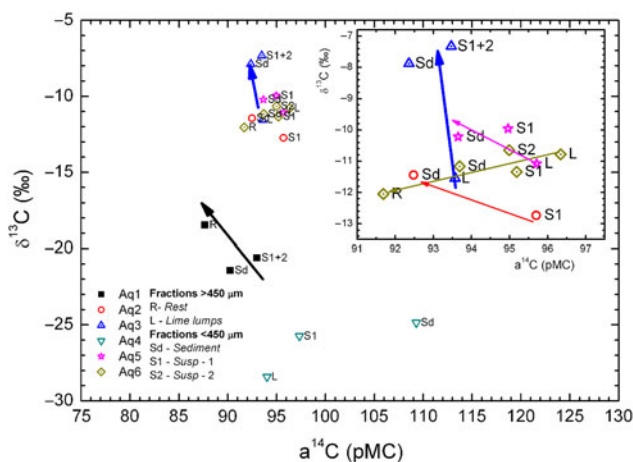


Figure 3 Relations between $a^{14}\text{C}$ and $\delta^{13}\text{C}$ for all analyzed fractions of each mortar sample. Insert shows enlarged area with data for samples Aq2, Aq3, Aq5, and Aq6; fractions: *Rest*- > 450 μm -bulk; *Sediment*- < 450 μm , precipitate after ultrasonification, *Susp*- < 450 μm , suspended part, (-1, CO_2 extracted within 60'; -2, CO_2 extracted till the end of reaction; -1 + 2, CO_2 extracted as bulk).

values (-28‰) it can be assumed for this fraction to be dead-carbon free and to give the date of a fire event. During delayed hardening process, after the fire, smaller particles could precipitate and would be extracted as *Susp* and *Sediment* fractions.

Aq6 $\delta^{13}\text{C}$ and $a^{14}\text{C}$ values do not indicate dead-carbon (limestone) contamination (Figure 3). As previously shown (examples Aq1, Aq4 and Ambers [1987]; Kosednar-Legenstein et al. [2008]), mortar carbonate can have a very low $\delta^{13}\text{C}$ value. In this case, it can be presumed that the building material for slaked lime was reused mortar, containing a mixture of non-reacted limestone ($a^{14}\text{C}$ of 0 pMC and $\delta^{13}\text{C}$ of 0‰) and anthropogenic carbonate (high $a^{14}\text{C}$ and low $\delta^{13}\text{C} \leq -20\text{‰}$). The mortar produced in this way would have *Lime lumps* reflecting the atmosphere (highest $a^{14}\text{C}$ and $\delta^{13}\text{C}$), while the *Rest* fraction would have lower $a^{14}\text{C}$ and $\delta^{13}\text{C}$, similar to a reused mortar.

Since the samples are expected to be from the same age, the similar ^{14}C dates are grouped together, focusing on the ages of the *Lime lumps*. Two distinctive ^{14}C age spans emerge: first from 584 ± 24 BP to 495 ± 21 BP (*Susp*-1 + 2 for Aq1 and Aq3 and *Lime lumps* for Aq3 and Aq4) and the second one from 353 ± 21 BP to 299 ± 21 BP (Aq2 *Susp*-1 and *Lime lumps* for Aq5 and Aq6).

Calibrating Dates of Mortar Samples

Calibrated ages for *Susp*-1 + 2 fractions of Aq1 and Aq3, *Susp*-1 of Aq2 and all *Lime lump* fractions of Aq3, Aq4, Aq5, and Aq6 are given in Figure 4. The assignment of the dates of construction is based on the ages of *Lime lump* fractions of Aq3 to Aq6 samples, and the ages of other fractions are associated based on the chi-square tests. Calibrated ages are reported for one σ range. Note that for the calibration of the two distinctive ^{14}C age spans, for the Combine function (OxCal v4.3.2, see Bronk Ramsey 2017) only the *Lime lumps*

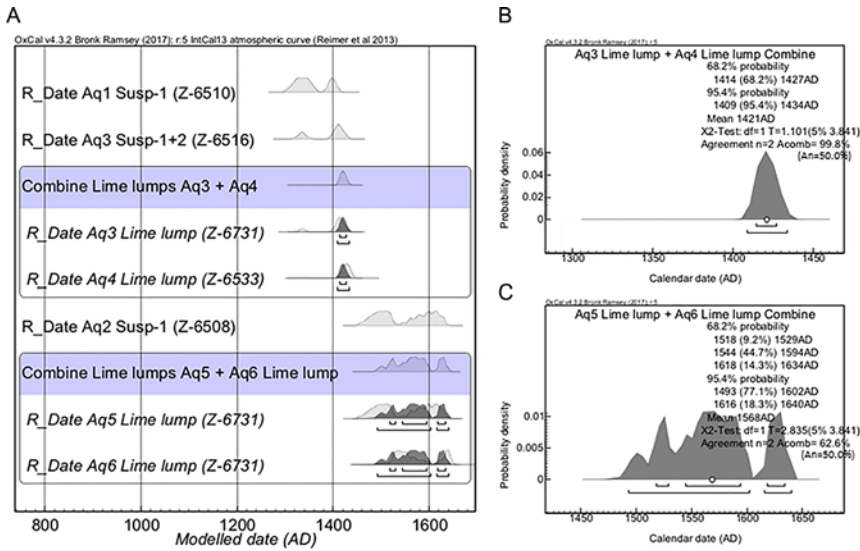


Figure 4 (A) Calibrated ages for *Susp-1 + 2* fractions of Aq1 and Aq3, *Susp-1* of Aq2 and Combine functions for Aq3 and Aq4 *Lime lumps* (with probability data in Figure 4B) and for Aq5 and Aq6 *Lime lumps* (with probability data in Figure 4C); fractions: *Susp-1* < 450 μm , suspended part, (-1, CO₂ extracted within 60'; -2, CO₂ extracted till the end of reaction; 1 + 2, CO₂ extracted in a bulk), *Lime lump* > 450 μm , white powdery lumps.

fractions were considered, since the *Susp* fractions were found unreliable in the most samples where it could be compared to *Lime lumps*.

Using the chi-square test, ages of *Susp* fractions of Aq1 and Aq3 and Aq3 *Lime lumps* are not significantly different, implying that the ages of Aq1 and Aq3 are the same. Also, *Lime lumps* of Aq3 and Aq4, are not significantly different, equaling the age of Aq4 to Aq3, i.e., to Aq1. Combine function for *Lime lumps* fractions of Aq3 and Aq4 gives date cal AD 1414–1427 (Figure 4B).

Similarly, chi-square test for *Susp* Aq2 and *Lime lumps* Aq5 and Aq6 fractions shows that they are not significantly different and the date for Aq2 can be associated with Aq5 and Aq6 dates.

Combine function for Aq5 and Aq6 *Lime lumps* fractions gives cal AD 1518–1529, 1544–1594, and cal AD 1618–1634 (Figure 4C).

One group of assembled samples—Aq1, Aq3, Aq4—collected from the Aqueduct foundation can all be dated to 15th century. Aq1 and Aq3 resembled on macroscopic morphology, also. Another group, Aq2, Aq5, and Aq6 resembled on the aggregate size (smaller than for Aq1 and Aq3), were all sampled from the non-degraded part of the Aqueduct and pointed to 16th and the first half of 17th century. However, considering these were preliminary results of mortar dating in the Zagreb Radiocarbon Laboratory and due to a low number of samples analyzed, it can be concluded that these samples belong to the period between 15th and 17th century.

CONCLUSION

We described the first attempt to date the mortar at the Ruđer Bošković Institute (Croatia) with the help from the Center for Applied Isotope Studies, University of Georgia, USA.

Non-hydraulic mortar from the Aqueduct from Skopje was sampled at 6 locations. A number of fractions were extracted using cryogenic breaking, lime lumps selection and ultrasonification. FTIR-ATR was used to qualitatively determine the chemical composition of fractions. The plausible dates were selected on the basis of ^{13}C to ^{14}C correlations and coinciding ^{14}C dates of the fractions predominantly based on the lime lump fractions. On the basis of morphology, sampling positions and calibrated ^{14}C ages, the samples were divided into two groups and were dated to the period between the 15th and 17th century.

ACKNOWLEDGMENTS

The Executive project design for conservation and restoration of the Aqueduct in Skopje (2014) is gratefully acknowledged for the financial support. FTIR-ATR was acquired through the Croatian Science Foundation (grant no. 9310). Thanks to Dr.sc. Ivanka Lovrenčić Mikelić for help with geological issues. We are especially thankful for the suggestions of the two anonymous reviewers.

REFERENCES

- Ambers J. 1987. Stable carbon isotope ratios and their relevance to the determination of accurate radiocarbon dates for lime mortars. *Journal of Archaeological Science* 14:569–576.
- Balabanov K, Kikolovski A, Kornakov D. 1980. Spomenici na kulturata na Makedonija [Monuments of culture in Macedonia]. Skopje, Macedonia: Mislra. p. 197. In *Macedonian*.
- Baxter MS, Walton A. 1970. Radiocarbon dating of mortars. *Nature* 225(5236):937–938.
- Bronk Ramsey C. 2016. The OxCal program v 4.2. The Oxford Radiocarbon Accelerator Unit, University of Oxford. Available at: <https://c14.arch.ox.ac.uk/oxcal/OxCal.html>.
- Bronk Ramsey C. 2017. OxCal v4.3.2 r:5. The Oxford Radiocarbon Accelerator Unit, University of Oxford. Available at: <https://c14.arch.ox.ac.uk/oxcal/OxCal.html>.
- Carmine L, Caroselli M, Lugli S, Marzaioli F, Nonni S, Marchetti S, Dori M, Terrasi F. 2015. AMS radiocarbon dating of mortar: the case study of the medieval UNESCO site of Modena. *Nuclear Instruments and Methods in Physics Research B* 361:614–619.
- Chu V, Regev L, Weiner S, Boaretto E. 2008. Differentiating between anthropogenic calcite in plaster, ash and natural calcite using infrared spectroscopy: implications in archaeology. *Journal of Archaeological Science* 35:905–911.
- Czernik J, Goslar T, Hayen R, Van Strydonck M, Fontaine L, Boudin M, Maspero F, Panzeri L, Galli A, Urbanova P, Guibert P. 2017. Preparation and dating of mortar samples—Mortar Dating Inter-comparison Study (MODIS). *Radiocarbon* 59(6):1845–1858.
- Fabbri B, Gualtieri S, Shoval S. 2014. The presence of calcite in archeological ceramics. *Journal of the European Ceramic Society* 34:1899–1911.
- Goslar T, Nawrocka D, Czernik J. 2009. Foraminiferous limestone in ^{14}C dating of mortar. *Radiocarbon* 51(3):987–993.
- Hale J, Heinemeier J, Lancaster L, Lindroos A, Ringbom Å. 2003. Dating ancient mortar. *American Scientist* 91:130–137.
- Hajdas I, Lindroos A, Heinemeier J, Ringbom Å, Marzaioli F, Terrasi F, Passariello I, Capano M, Artioli G, Addis A, Secco M, Michalska D, Czernik J, Goslar T, Hayen R, Van Strydonck M, Fontaine L, Boudin M, Maspero F, Panzeri L, Galli A, Urbanova P, Guibert P. 2017. Preparation and dating of mortar samples—Mortar Dating Inter-comparison Study (MODIS). *Radiocarbon* 59(6):1845–1858.
- Hayen R, Van Strydonck M, Boaretto E, Lindross A, Heinemeier J, Ringbom A, Hueglin S, Michalska D, Hajdas I, Marzaioli F, Maspero F, Galli A, Artioli G, Moreau Ch, Guibert P, Caroselli M. 2016. Absolute dating of mortars – integrating chemical and physical techniques to characterize and select the mortar samples. In: Papayianni I, Stefanidou M, Pachta V, editors. *HMC2016, Greece*. ISBN 978-960-99922-3-7. p. 656–667.
- Hayen R, Van Strydonck M, Fontaine L, Boudin M, Lindross A, Heinemeier J, Ringbom A, Michalska D, Hajdas I, Hueglin S, Marzaioli F, Terrasi F, Passariello I, Capano M, Artioli G, Addis A, Secco M, Maspero F, Panzeri L, Galli A, Guibert P, Urbanová P, Czernik J, Goslar T, Caroselli M. 2017. Mortar dating methodology: assessing recurrent issues and needs for further research. *Radiocarbon* 59(6):1859–1871.
- Heinemeier J, Ringbom A, Lindroos A, Sveinbjornsdottir A E. 2010. Successful AMS ^{14}C dating of non-hydraulic lime mortars from the medieval churches of the Aland Islands, Finland. *Radiocarbon* 52(1):171–204.

- Kabacińska Z, Krzymiński R, Michalska D, Dobosz B. 2014. Investigation of lime mortars and plasters from archaeological excavations in Hippos (Israel) using electron paramagnetic resonance. *Geochronometria* 41(2):112–120.
- Kosednar-Legenstein B, Dietzel M, Leis A, Stingl K. 2008. Stable carbon and oxygen isotope investigation in historical lime mortar and plaster—results from field and experimental study. *Nuclear Instruments and Methods in Physics Research B* 331:220–224.
- Krajcar Bronić I, Horvatinčić N, Sironić A, Obelić B, Barešić J, Felja I. 2010. A new graphite preparation line for AMS ^{14}C dating in the Zagreb Radiocarbon Laboratory. *Nuclear Instruments and Methods in Physics Research B* 268 (7/8):943–946.
- Kumbaradžić-Bogojević L. 1998. Osmanliki spomenici vo Skopje [Ottoman monuments in Skopje]. Skopje, Macedonia: IZRM. p. 60. In Macedonian.
- Labeyrie J, Delibrias G. 1964. Dating of old mortars by the carbon-14 method. *Nature* 201(4920):742.
- Lindroos A, Heinemeier J, Ringbom Å, Braskén M, Sveinbjörnsdóttir ÁE. 2007. Mortar dating using AMS ^{14}C and sequential dissolution: examples from medieval, non-hydraulic lime mortars from the Åland Islands, SW Finland. *Radiocarbon* 49(1):47–67.
- Lindroos A, Regev L, Oinonen M, Ringbom Å, Heinemeier J. 2012. ^{14}C dating of fire damaged mortars from medieval Finland. *Radiocarbon* 54(3–4):915–931.
- Lindroos A, Ranta H, Heinemeier J, Lill J-O. 2014. ^{14}C chronology of the oldest Scandinavian church in use. An AMS/PIXE study of lime lump carbonate in mortar. *Nuclear Methods and Instruments in Physics Research B* 331:220–224.
- Lindroos A, Ringbom A, Heinemeier J, Hodgins G, Sonck-Koota P, Sjöberg P, Lancaster L, Kaisti R, Brock F, Ranta H, Caroselli M, Lugli S. 2018. Radiocarbon dating historical mortars: Lime lumps and/or binder carbonate. *Radiocarbon* 60(3):875–899.
- Marzaioli F, Nonni S, Passariello I, Capano M, Ricci P, Lubritto C, De Cesare N, Eramo G, Quirós Castillo JA, Terrasi F. 2013. Accelerator mass spectrometry ^{14}C dating of lime mortars: methodological aspects and field study applications at CIRCE. *Nuclear Instruments and Methods in Physics Research B* 294:246–251.
- Michalska D, Czernik J. 2015. Carbonates in leaching reactions in context of ^{14}C dating. *Nuclear Instruments and Methods in Physics Research B* 361:431–439.
- Michalska Nawrocka D, Micheżyńska DJ, Pazdur A, Czernik J. 2007. Radiocarbon chronology of the ancient settlement on the Golan Heights. *Radiocarbon* 49(2):625–37.
- Michalska D, Pazdur A, Czernik J, Szczepaniak M, Żurakowska M. 2013. Cretaceous aggregate and reservoir effect in dating of binding materials. *Geochronometria* 40(1):33–41.
- Michalska D, Czernik J, Goslar T. 2017. Methodological aspect of mortars dating (Poznań, Poland, MODIS). *Radiocarbon* 59(6): 1891–1906.
- Mook WG, van der Plicht J. 1999. Reporting ^{14}C activities and concentrations. *Radiocarbon* 41:227–239.
- Nawrocka D, Pawlita J, Pazdur A. 2005. Application of radiocarbon method for dating of lime mortars. *Journal on Methods and Applications of Absolute Chronology Geochronometria* 24: 109–115.
- Nonni S, Marzaioli F, Secco M, Passariello I, Capano M, Lubritto C, Mignardi S, Tonghini C, Terrasi F. 2013. ^{14}C mortar dating: The case of medieval Shayzar citadel, Syria. *Radiocarbon* 55(2–3): 514–525.
- Nonni S, Marzaioli F, Mignardi S, Passariello I, Capano M, Terrasi F. 2018. Radiocarbon dating of mortars with a pozzolana aggregate using the Cryo2Sonic protocol to isolate the binder. *Radiocarbon* 60(2):617–637.
- Ortega LA, Zuluaga MC, Alonso-Olazabal A, Insausti M, Ibañez A. 2008. Geochemical characterization of archaeological lime mortars: Provenance inputs. *Archaeometry* 50:387–408.
- Ortega LA, Zuluaga MC, Alonso-Olazabal A, Murelaga X, Insausti M, Ibañez A. 2012. Historic lime-mortar ^{14}C dating of Santa María La Real (Zarautz, northern Spain). *Radiocarbon* 54:23–36.
- Pesce GLA, Ball RJ. 2012. Dating of old lime based mixtures with the “Pure Lime Lumps” technique. *Radiometric dating*. In: Michalska Nawrocka D, editor. InTech. Available at: <https://www.intechopen.com/books/radiometric-dating/dating-of-old-lime-based-mixtures-with-the-pure-lime-lumps-technique>.
- Pesce GLA, Quarta G, Calganile L, D’Elia MD, Cavaciocchi P, Iastrico C, Guastella R. 2009. Radiocarbon dating of lumps from aerial mortars and plasters: methodological issues and results from San Nicolò of Capodimonte church (Camogli, Genoa, Italy). *Radiocarbon* 51(2):867–872.
- Petr V. 1998. Akveduktot kraj Skopje i problemot na negovoto datiranje [Problems of dating the Skopje Aqueduct]. *Makedonsko nasledstvo (MakNas)* 7:87–111. In Macedonian.
- Poduska KM, Regev L, Berna F, Mintz E, Milevski I, Kahalailly H, Weiner S, Boaretto E. 2012. Plaster characterization at the PPNB site of Yiftahael (Israel) including the use of ^{14}C : implication for plaster production, preservation, and dating. *Radiocarbon* 54(3–4):887–896.

- Reimer PJ, Bard E, Bayliss A, Beck JW, Blackwell PG, Bronk Ramsey C, Buck CE, Cheng H, Edwards RL, Friedrich M, Grootes PM, Guilderson TP, Hafliðason H, Hajdas I, Hatté C, Heaton TJ, Hoffmann DL, Hogg AG, Hughen KA, Kaiser KF, Kromer B, Manning SW, Niu M, Reimer RW, Richards DA, Scott EM, Southon JR, Staff RA, Turney CSM, van der Plicht J. 2013. IntCal13 and Marine13 radiocarbon age calibration curves 0–50,000 years cal BP. *Radiocarbon* 55(4):1869–1887.
- Ringbom A, Heinemeier J, Lindroos A, Brock F. 2008. Mortar dating and Roman pozzolana, results and interpretations. *Comm. Hum. Litt.* 128:187–208.
- Ringbom Å, Lindroos A, Heinemeier J, Sonck-Koota P. 2014. 19 years of mortar dating: learning from experience. *Radiocarbon* 56(2) 619–635.
- Sironić A, Krajcar Bronić I, Horvatinčić N, Barešić J, Obelić B, Felja I. 2013. Status report on the Zagreb radiocarbon laboratory—AMS and LSC results of VIRI intercomparison samples. *Nuclear Instruments and Methods in Physics Research B* 294:185–188.
- Sonninen E, Erametsa P, Jungner H. 1989. Dating of mortar and bricks: an example from Finland. In: Maniatis Y, editor. *Archaeometry: proceedings of the 25th international symposium*. p. 99–107.
- Szczepaniak M, Nawrocka D, Mrozek-Wysocka M. 2008. Applied geology in analytical characterization of stone materials from historical building. *Applied Physics A: Materials Science & Processing* 90(1):89–95.
- Van Balen K. 2005. Carbonation reaction of lime, kinetics at ambient temperature. *Cement and Concrete Research* 35:647–657.
- Van Strydonck M, Dupas M. 1989. Isotopic fractionation of oxygen and carbon in lime mortar under natural environmental conditions. *Radiocarbon* 31(3):610–618.
- Van Strydonck M, Dupas M, Dauchot-Dehon M, Pachiaudi J. 1986. The influence of contaminating (fossil) carbonate and the variations of $\delta^{13}\text{C}$ in mortar dating. *Radiocarbon* 28(2A):702–710.